

Source waters and flow paths in an alpine catchment, Colorado Front Range, United States

Fengjing Liu, Mark W. Williams, and Nel Caine

Department of Geography and Institute of Arctic and Alpine Research, University of Colorado, Boulder, Colorado, USA

Received 4 February 2004; revised 2 June 2004; accepted 24 June 2004; published 9 September 2004.

[1] Source waters and flow paths of streamflow draining high-elevation catchments of the Colorado Rocky Mountains were determined using isotopic and geochemical tracers during the 1996 snowmelt runoff season at two subcatchments of the Green Lakes Valley, Colorado Front Range. A two-component hydrograph separation using $\delta^{18}\text{O}$ indicates that new water dominated ($82 \pm 6\%$) streamflow at the 8-ha Martinelli catchment and old water dominated ($64 \pm 2\%$) at the 225-ha Green Lake 4 (GL4) catchment. Snowmelt became isotopically enriched as the melt season progressed, complicating the interpretation of source water models. Thus old water may be underestimated if the temporal variation in $\delta^{18}\text{O}$ of snowmelt is ignored or extrapolated from point measurements to the catchment. Two-component hydrograph separations for unreacted and reacted waters using a single geochemical tracer were not always meaningful. Three-component hydrograph separations using end-member mixing analysis indicated that subsurface flow contributed more than two thirds to the streamflow at both catchments. Talus fields contributed more than 40% of the total discharge during summer at the GL4 catchment. A conceptual model was established for flow generation based on these results. It is suggested that surface water and groundwater interactions are much more important to the quantity and quality of surface water in high-elevation catchments than previously thought. *INDEX TERMS*: 1806 Hydrology: Chemistry of fresh water; 1829 Hydrology: Groundwater hydrology; 1871 Hydrology: Surface water quality; *KEYWORDS*: alpine catchment, end-member mixing analysis, flow paths, mixing model, source waters

Citation: Liu, F., M. W. Williams, and N. Caine (2004), Source waters and flow paths in an alpine catchment, Colorado Front Range, United States, *Water Resour. Res.*, 40, W09401, doi:10.1029/2004WR003076.

1. Introduction

[2] It is important to understand flow sources and pathways that control water quantity and quality in streamflows draining high-elevation catchments in Colorado. The Front Range of Colorado and its extension into southern Wyoming receives as much as $7 \text{ kg ha}^{-1} \text{ yr}^{-1}$ of atmospheric nitrogen (N) deposition, an amount that may have caused changes in aquatic and terrestrial life in otherwise pristine ecosystems [Burns, 2002]. Nitrogen saturation appears to be occurring throughout high-elevation catchments of the Colorado Front Range and may be affecting water quality [Baron et al., 1994; Williams et al., 1996a; Williams and Tonnessen, 2000; Baron et al., 2000]. S. B. Waters et al. (Algal responses to nutrient and climate fluctuations in an alpine lake, Colorado, USA, submitted to *Journal of Phycology*, 2004) have shown that increased atmospheric deposition of inorganic N in the last 40 years has changed the flora of Green Lake 4. Other analyses of high-elevation lake sediment cores from Rocky Mountain National Park [Wolfe et al., 2001] show increased algal productivity attributed to nutrient enrichment from atmospheric N deposition. These results suggest that current levels of N deposition are sufficient to alter both the quantity and quality of

organic matter in Colorado alpine lakes. However, the sources and sinks of N in these watersheds are not well known at this time because of a lack of knowledge of flow sources and pathways [Campbell et al., 1995; Burns, 2002].

[3] The identification of flow sources and pathways is crucial for understanding the links between terrestrial and aquatic ecosystems [Cirimo and McDonnell, 1997; Holko and Lepisto, 1997; Perakis, 2002]. Soil and groundwater chemical and isotopic analyses have been used to provide quantitative, multicomponent mass balance models of streamflow during snowmelt at watersheds in eastern North America [Wels et al., 1990]; but generally such models have not been well developed for watersheds of the Colorado Rocky Mountains, in part, due to the difficulty of access during snowmelt. Further advances in understanding the sources and sinks of N during snowmelt will require the development of multicomponent runoff models that utilize solute and isotopic measurements of source waters [Burns, 2002].

[4] There has been little emphasis on the challenges of hydrograph separation in seasonally snow-covered catchments [Laudon et al., 2002]. In the past, depth integrated snow cores have been used to define the event component during snowmelt runoff [Rodhe, 1981; Bottomley et al., 1986; Ingrahan and Taylor, 1989]. Recent findings have shown a systematic variation in the isotopic composition of snowmelt caused by fractionation of the meltwater as it

percolates through the snowpack [Taylor *et al.*, 2001; Unnikrishna *et al.*, 2002]. Taylor *et al.* [2002] show that the temporal variation of $\delta^{18}\text{O}$ in snowmelt is on the order of 4‰ for a variety of catchments in maritime and continental climates. An outstanding question is how to account for this change in the isotopic content of meltwater over time in seasonally snow covered catchments and how to accommodate it in mixing models [Rodhe, 1987; Sueker *et al.*, 2000; Laudon *et al.*, 2002].

[5] Our objective here is to improve our understanding of source waters and flow paths in seasonally snow covered alpine catchments where discharge is dominated by snowmelt runoff. For data collected in 1996 we evaluate the advantages, disadvantages, and insights into source waters and flow paths provided by two- and three-component models of hydrograph separation in two basins of the Green Lakes Valley in the Colorado Front Range, the 8-ha Martinelli catchment and the 225-ha Green Lakes Valley above the outlet of Green Lake 4. End-member mixing analysis (EMMA) [Christophersen *et al.*, 1990; Hooper *et al.*, 1990] was used for three-component hydrograph separations. Specific questions addressed are: (1) What is the magnitude of $\delta^{18}\text{O}$ fractionation in snowmelt runoff? (2) How do we extrapolate information on $\delta^{18}\text{O}$ fractionation measured in snowmelt lysimeters to the basin scale? (3) How does the amount of “event” water change as basin size increases from 8 ha to 225 ha? (4) What role does groundwater play in the discharge of alpine streams? (5) What, if any, is the role of talus fields in streamflow quantity and quality? We then use this information to develop a conceptual model of source waters and flow paths for these two catchments.

2. Site Description

[6] The Colorado Front Range rises directly from the Denver-Boulder-Fort Collins metropolitan area. This geographical setting results in high-elevation basins of this portion of the Continental Divide being located just west of large urban and agricultural activities. Green Lakes Valley (40°03'N, 105°35'W) is an east facing headwater catchment, about 700 ha in area, and ranging in elevation from 3250 m to about 4000 m at the Continental Divide (Figure 1). Bedrock underlying the lower valley is dominated by granites and quartz monzonites of two different intrusions: the Silver Plume monzonite of Precambrian age and the Audubon-Albion stock of Miocene age [Caine and Thurman, 1990]. The Silver Plume monzonite extends into the upper valley. The catchment is typical of the high-elevation environment of the Colorado Front Range with long, cool winters and a short growing season (1–3 months) [Williams *et al.*, 1996b]. The catchment includes Niwot Ridge (Figure 1), where research has been conducted since the early 1950's [Caine and Thurman, 1990]. This site is a Long-Term Ecological Research (LTER) network site. The Green Lakes Valley is a water source for the city of Boulder and public access is prohibited.

[7] For this study we focus on the catchment above Green Lake 4 (GL4) and the Martinelli catchment. The GL4 catchment extends to the Continental Divide at an elevation slightly above 4,000 m and drains an area of 225 ha at the outlet of the lake at an elevation of 3515 m (Figure 1). The catchment is characterized by steep rock walls and coarse debris, and a valley floor of glaciated bedrock. About 20%

of the basin is covered by vegetation with well-developed soil, most of which is located in the valley bottom. Soils are Cryic entisols and inceptisols on hillslopes, with histosols found on wetter sections of the valley floor [Williams *et al.*, 2001]. Coarse debris, including talus slopes, blockslopes, and rock glaciers, cover about 45% of the GL4 catchment. This coarse debris is poorly sorted, generally unconsolidated and includes a range of particle sizes from clays to boulders more than 2 m in diameter [Williams *et al.*, 1997]. Talus slopes are usually overlain by blockslopes on their top or foot, which form through freeze/thaw weathering of bedrock and are less consolidated compared to talus slopes. Here we use the term “talus field” as a shorthand for coarse debris slopes. Three streams draining talus fields on the east face of Niwot Ridge (Figure 1) (EN (east Niwot) 1, 2, and 4 going from east to west) were sampled on the upper portion of the slope (U), in the middle portion of the slope (M), and in the lower portion of the slope (L), with some streams also sampled where the talus fields joined the valley bottom (V).

[8] The 8-ha Martinelli catchment is located about 400 m from the Saddle site on Niwot Ridge; the outlet is at an elevation of 3380 m (Figure 1). The Martinelli catchment has a poorly developed soil structure, little vegetation, and a deep winter snow cover [Caine, 1989].

[9] Niwot Ridge, the northern boundary of the Green Lakes Valley, is the site of other experimental areas, including snow lysimeters, a subnivean laboratory and an Aerometrics wet-chemistry precipitation collector at the Saddle site (Figure 1), as part of the National Atmospheric Deposition Program (NADP).

3. Methods

3.1. Sample Collection

3.1.1. Snow

[10] Physical and chemical properties of snow were routinely measured on a weekly basis at the Saddle site using sampling protocols presented by Williams *et al.* [1996c, 1999]. Snowpack meltwater was collected in 1-m² snow lysimeters before contact with the ground. Snowmelt flowed by gravity from the snow lysimeters about 5 m into a subnivean laboratory, where grab samples were collected approximately daily for solute chemistry and stable water isotope analysis. Additionally, an annual snow survey was conducted in the Green Lakes Valley at maximum snow accumulation to measure the spatial distribution of snow quantity and quality [Winstral *et al.*, 2002; Williams *et al.*, 1999; Williams *et al.*, 2001]. Thirteen snow pits were sampled on 23–24 April (calendar day 114–115) of 1996 for solute content and stable water isotopes (Figure 1).

3.1.2. Rain

[11] The Niwot Ridge/Green Lakes Valley LTER site participates in the National Atmospheric Deposition Program (NADP), which operates about 200 wet precipitation collectors throughout the continental United States. Splits of the NADP samples were analyzed for solute content and stable water isotopes, as described by Williams *et al.* [2001].

3.1.3. Surface Waters

[12] Seasonal discharge has been measured continuously since about 1982 at both catchments from about 1 May to 30 October [Williams and Caine, 2002]. Streams and subtalus water were sampled as grab samples. Polyethylene bottles were soaked with DI water overnight and then rinsed

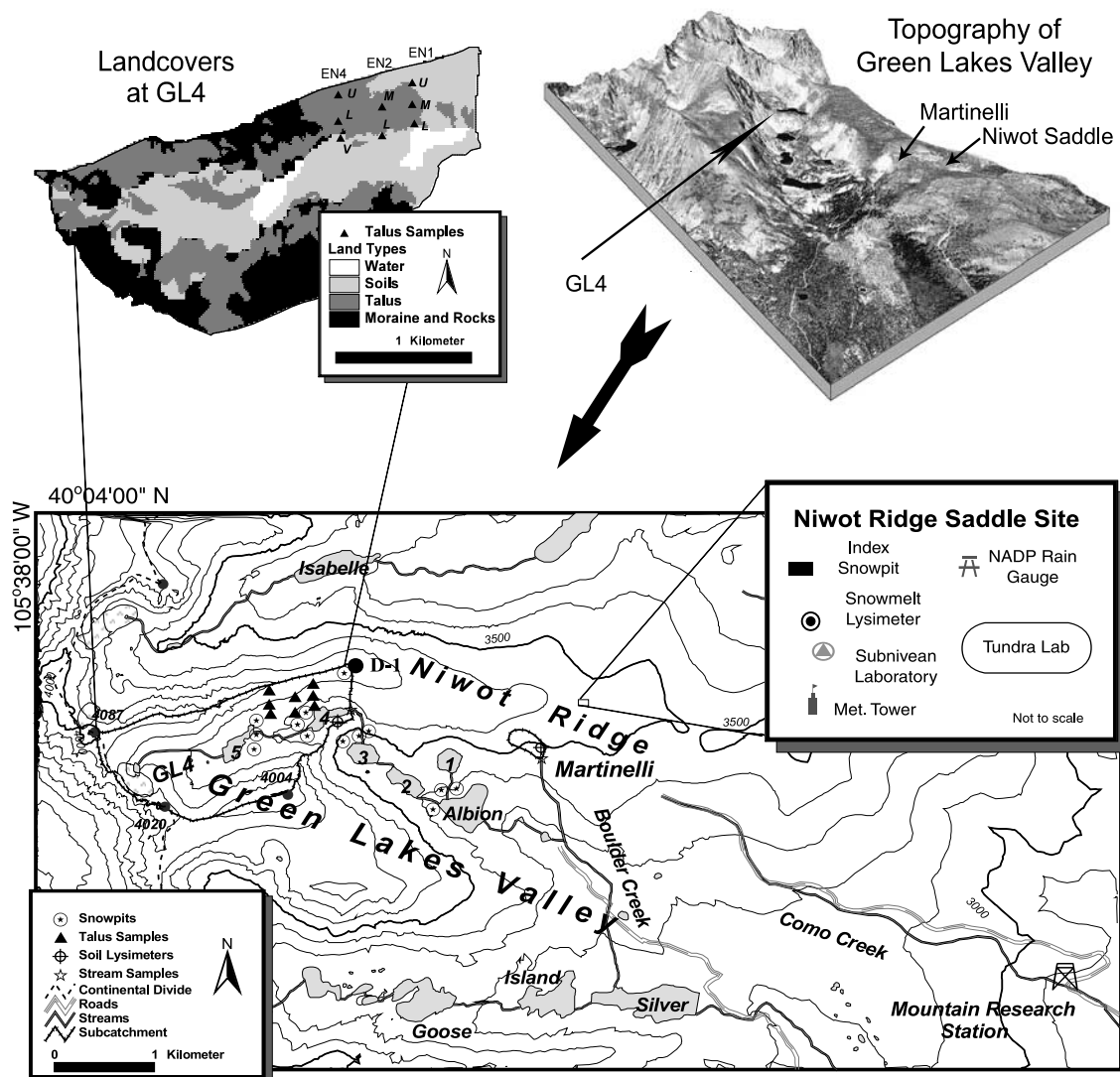


Figure 1. Location map of the Martinelli and the GL4 catchments, including the Saddle site on Niwot Ridge. Sampling sites are indicated for discharge, snow, snowmelt before contact with the ground, soil water, and talus water.

with DI water five times; bottles were further rinsed three times with sample water at the time of collection. Stream samples were collected weekly starting with the initiation of snowmelt runoff and monthly during the nonmelt season at GL4. Subtalus water samples were collected as a time series at 8 sites from about the end of snowmelt as sites became accessible to the end of August (n at each site ranged from 3 to 9) [Williams *et al.*, 1997]. All water samples were transported the same day as collection to our wet chemistry laboratory and treated as the snow samples.

3.1.4. Soil Lysimeters

[13] Zero-tension soil lysimeters, constructed of halved 400-mm sections of PVC pipe 250 mm in diameter, capped on one end, and plumbed to drain into a 1-L storage bottle connected to the surface with tygon tubing, were installed in the mid-1980s [Litaor, 1993]. At the GL4 catchment, 4 zero-tension soil lysimeters were installed along a hill-slope catena with a northwestern aspect located with the bottom site just above lake level and about 20 m from the

lake (Figure 1). At the Martinelli catchment, 25 zero-tension lysimeters were installed on 5×5 array located about 100 m from the gaging site (Figure 1), but spacing is ~ 1 m separation along contours and 5 m between plots along slope. Sample collection started when an area became snow free and continued at weekly to biweekly intervals. After the end of snowmelt, the soil lysimeters rarely contained water except after rain events.

3.2. Laboratory Analyses

[14] All water and snow samples were analyzed for pH, acid neutralizing capacity (ANC), conductance, major ions and dissolved silica (Si), following the protocols presented by Williams *et al.* [1996c]. Snow samples were stored frozen (-20°C) for 1–2 months until analysis. Snow samples were placed in covered polyethylene buckets and melted at room temperature. ANC was measured immediately after melting for snow or on submission to the laboratory by the Gran titration. As Neal [2001] noted, the Gran titration may

underestimate ANC, particularly in lower pH (<4.5). Since pH in our water is usually around 6 or 7 [Caine and Thurman, 1990], it's believed that this underestimation should be insignificant. Subsamples were immediately filtered through prerinsed (300 mL), 47-mm Gelman A/E glass fiber filters with an approximately 1- μ m pore size. Filtered samples were stored in the dark at 4°C for subsequent analyses of major anions using a Dionex DX 500 ion chromatograph and cations using a Varian AA6 atomic absorption spectrophotometer within 1–4 weeks. Analytical precision for all solutes was less than 2% and detection limit was less than 1 μ eq L⁻¹ [Williams and Caine, 2002].

[15] Isotope samples were collected in 30-mL borosilicate vials with airtight caps. Analyses for $\delta^{18}\text{O}$ were performed at the USGS Isotope Laboratory in Menlo Park, California. The 1 σ precision was $\pm 0.05\%$ based on replicate samples. Isotopic compositions are expressed as a δ (per mil) ratio of the sample to the Vienna Standard Mean Ocean Water (VSMOW) standard, where R is the ratio of $^{18}\text{O}/^{16}\text{O}$:

$$\delta^{18}\text{O}_{\text{sample}} = [(R_{\text{sample}}/R_{\text{VSMOW}}) - 1] \times 10^3 \quad (1)$$

3.3. Hydrograph Separations

[16] The new and old water components were estimated using $\delta^{18}\text{O}$ by [e.g., Sklash et al., 1976; Hooper and Shoemaker, 1986]

$$Q_s \times C_s = Q_n \times C_n + Q_o \times C_o \quad (2)$$

$$Q_s = Q_n + Q_o \quad (3)$$

where Q is volume flow rate, C is $\delta^{18}\text{O}$ content, and the subscripts describe the water source (s is stream water, n is new water, and o is old water).

[17] Recent focus of hydrograph separation has been on uncertainty analysis. Several approaches are available for calculating uncertainty, e.g., Bayesian statistical method [Soulsby et al., 2003], Monte Carlo procedure [Joerin et al., 2002], and Gaussian error propagation technique [Genereux, 1998; Uhlenbrook and Hoeg, 2003]. For this study, the explicit equation from Gaussian error propagation technique was used for two-component hydrograph separations following Genereux [1998]:

$$W_{f_n} = W_{f_o} = \left\{ \left[\frac{f_o}{(C_n - C_o)} W_{C_o} \right]^2 + \left[\frac{f_n}{(C_n - C_o)} W_{C_n} \right]^2 + \left[\frac{-1}{(C_n - C_o)} W_{C_s} \right]^2 \right\}^{\frac{1}{2}} \quad (4)$$

In this equation, fraction of total streamflow due to a component (f) is used instead of Q in order to simplify the calculation. W is uncertainty, and all W terms in the right side of equation represent term uncertainty due to spatial and temporal variation of $\delta^{18}\text{O}$ in the two components.

[18] Equations (2)–(4) were also used to determine reacted and unreacted components by substituting geochemical tracers for $\delta^{18}\text{O}$ and unreacted and reacted waters for new and old waters [Sueker et al., 2000]. Several conditions must be met for this two-component model, including [e.g., Buttle, 1994]: (1) Tracer values of each component must be

significantly different; (2) there are only two components contributing to streamflow; and (3) the tracer composition of each component is constant for the duration of the event, or variation is known from measurements.

[19] End-member mixing analysis (EMMA) was used to determine proportions of end-members contributing to streamflow, following the procedures of Christophersen and Hooper [1992]. Streamflow samples and end-members were standardized for all conservative tracers using the mean and standard deviation of streamflow following the procedure of Hooper [2003] and Burns et al. [2001].

[20] Note that it is possible for some samples to lie outside the domain defined by the selected end-members. If this occurs, solutions should have negative fractions for some end-members, which are not realistic. To solve this problem, negative fractions were forced to zero and the other fractions were resolved by a geometrical approach, following the notion of Christophersen et al. [1990] and Hooper et al. [1990] (Appendix A).

4. Results

4.1. Hydrology

[21] Annual precipitation in the water year 1996 was slightly above normal, at 1,186 mm compared to the 50-year mean of 1,000 mm [Williams et al., 1996b]. Summer rainfall contributed approximately 15% of the annual precipitation in 1996. Precipitation in the water year 1995 was 1582 mm, about 160% of the average precipitation since 1951. The relatively wet year in 1995 may have resulted in higher antecedent soil moisture at the start of runoff in 1996.

[22] Hydrographs at both the Martinelli (Figure 2c) and GL4 (Figure 2f) catchments are characteristic of snowmelt-dominated watersheds. The steep rising limb was driven by snowmelt runoff in May and June. The rising limb can be divided into two parts: (1) a small increase in discharge during the first 20 days of snowmelt and (2) a very rapid increase in discharge starting on about day 155. The recession limb was relatively long and gradual, with small increases in discharge from summer rains. Annual discharge was about 100% of the 20-year average at the GL4 catchment but about 150% at the Martinelli catchment.

4.2. Solute Content

[23] Changes of solute concentrations over time in both streams followed a similar pattern (Figure 2). Concentrations were generally higher during the first 20 days of snowmelt. With the rapid increase in discharge on day 155, solute concentrations began to decrease. Annual minimum concentrations of all solutes occurred just after maximum discharge near day 190. Solute concentrations began to increase on the recession limb of the hydrograph.

[24] Box plots showing the median and quartiles of selected solutes are presented in Figure 3 for snow, snowmelt, stream waters, soil lysimeters, and talus waters. Solute concentrations in snow pits and meltwater were generally lower than other types of water. Concentrations in talus waters varied widely, with a general trend to higher concentrations from sites lower on slopes.

4.3. Water Isotopes

[25] The $\delta^{18}\text{O}$ of precipitation was depleted in snow and relatively enriched in summer rain (Figure 4). The $\delta^{18}\text{O}$

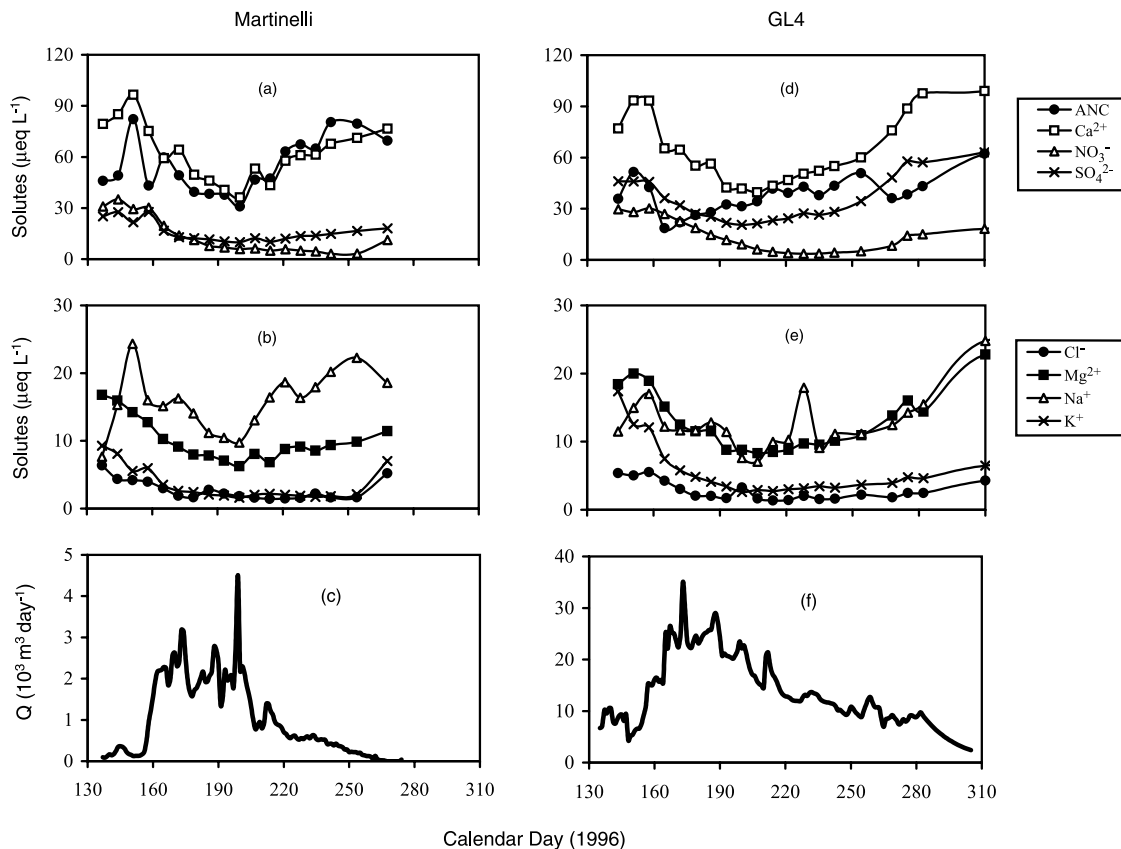


Figure 2. Time series from 1996 of discharge and solute concentrations from the Martinelli and GL4 catchments.

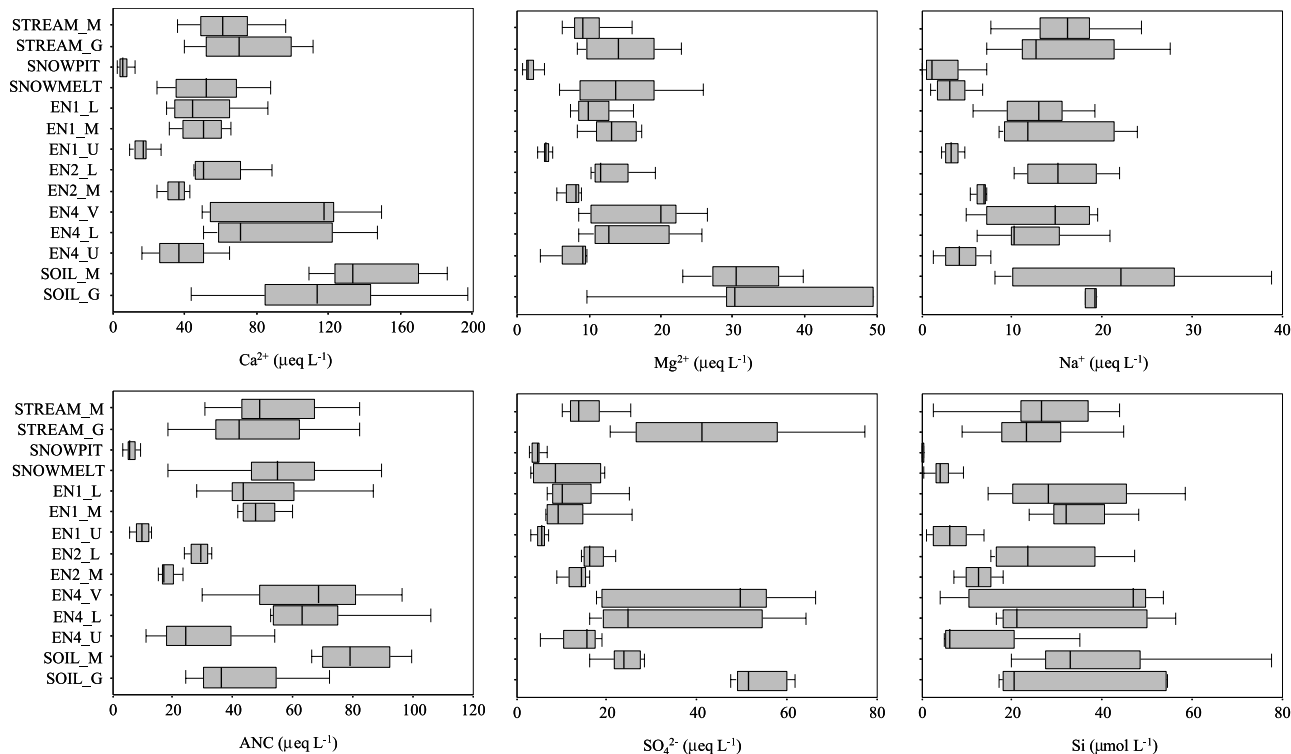


Figure 3. Box plots showing median and quartiles (25% and 75% and 5% and 95%) for selected solute concentrations in streamflow of 1996 (STREAM_M is for Martinelli and STREAM_G is for GL4), snow pit, snowmelt, talus waters (EN1, 2, and 4), and zero-tension soil lysimeters (SOIL_M is for Martinelli and SOIL_G is for GL4).

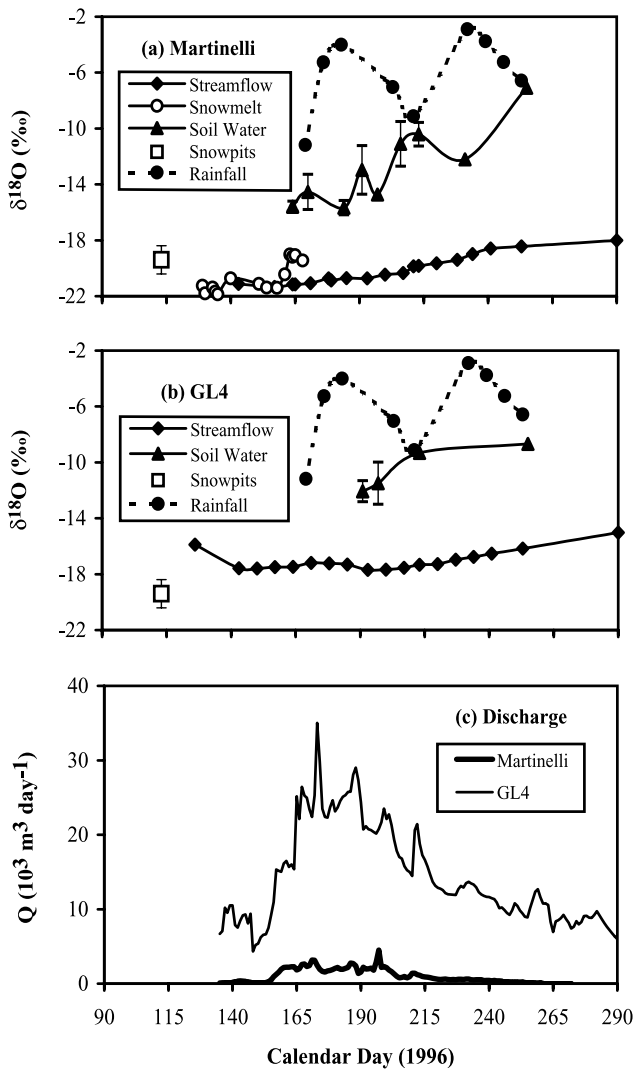


Figure 4. Time series of $\delta^{18}\text{O}$ values in streamflow, snowmelt, rainwater, and zero-tension soil lysimeters at (a) Martinelli and (b) GL4 catchment, along with (c) discharge. Mean $\delta^{18}\text{O}$ values are also shown from the synoptic snow survey on days 113–114. Error bars are shown as $\pm 1\sigma$ where more than one sample per day was collected.

value for bulk snow samples from 13 snow pits collected in the Green Lakes Valley on days 114 and 115 at maximum snow accumulation was $-19.4 \pm 1.0\text{‰}$. The bulk value of the index snow pit sampled at the snow lysimeter site on day 114 was -20.1‰ , within one standard deviation of the mean $\delta^{18}\text{O}$ value for snow in the Green Lakes Valley. Summer rains were enriched relative to snow values, with a maximum value of -2.9‰ occurring on day 232.

[26] The $\delta^{18}\text{O}$ of snowmelt became enriched with time, ranging from -21.9‰ , near the start of snowmelt to -18.0‰ , at the end of snowmelt on day 171 (Figure 4). Over the course of snowmelt, the $\delta^{18}\text{O}$ value increased by almost 4‰ . Both the arithmetic mean (-20.0‰) and volume-weighted mean (-20.3‰) of the 14 measured values in snowmelt were very close to the value of -20.1‰ measured in the index snow pit at maximum accumulation.

[27] The $\delta^{18}\text{O}$ values in the streamflow at the Martinelli catchment became more enriched with time, from -21.3‰ at the initiation of seasonal runoff to -18.0‰ on day 290 (Figure 4), a difference of 3.3‰ . The arithmetic mean of -20.2‰ for the Martinelli stream was very close to the snowpack value of -20.1‰ at the index snow pit and the arithmetic mean of -20.0‰ for snowmelt. However, the range in $\delta^{18}\text{O}$ values for the Martinelli drainage of 3.3‰ was 0.7‰ less than that in snowmelt collected at the Saddle, 400 m away from the Martinelli catchment.

[28] The $\delta^{18}\text{O}$ values in the streamflow at the GL4 catchment showed a similar pattern but with higher values compared to the Martinelli catchment. Prior to the initiation of intensive snowmelt runoff on day 126, $\delta^{18}\text{O}$ value was -15.9‰ . The $\delta^{18}\text{O}$ value then dropped by almost 2‰ to -17.6‰ on day 143. The $\delta^{18}\text{O}$ values then became more enriched with time, returning to near base flow values at -16.2‰ on day 253. The range in $\delta^{18}\text{O}$ values for the GL4 catchment of 2.6‰ was less than the range of 3.3‰ for the Martinelli catchment.

[29] The $\delta^{18}\text{O}$ values from soil solution were enriched relative to snow and stream water samples (Figure 4). The first samples were collected in June when sites became snow-free, providing access to the soil lysimeters. The soil lysimeters became dry in early July and we were only able to collect samples after rain events. At the Martinelli site, the $\delta^{18}\text{O}$ values ranged from -16‰ on day 160 to -7‰ on day 255. Similarly, at the GL4, the $\delta^{18}\text{O}$ values ranged from -12‰ on day 190 to -9‰ on day 255. The $\delta^{18}\text{O}$ values from soil lysimeters were always enriched more than 5‰ compared to stream water on the same day.

4.4. Two-Component Mixing Model: Source Waters

[30] New water and old water are defined using the time source definitions developed by Sklash *et al.* [1976] and Hooper and Shoemaker [1986]. Old water is defined as water stored in the basin prior to the initiation of snowmelt and new water is that year's snowmelt runoff. Two methods were evaluated for parameterizing old water (Table 1): (1) using the $\delta^{18}\text{O}$ values from soil lysimeters that varied over time and (2) using base flow $\delta^{18}\text{O}$, temporally invariant. Note that base flow was actually parameterized by the last streamflow sample collected on day 290 of 1996 at both catchments. Temporal variation of $\delta^{18}\text{O}$ in streamflow tends to have a trough shape (Figure 4b). Streamflow samples collected prior to the initiation of intensive snowmelt such as the sample on day 126 at the GL4 catchment may contain some meltwater. New water was parameterized in four ways: (1) bulk $\delta^{18}\text{O}$ value of the index snow pit at maximum accumulation, (2) mean $\delta^{18}\text{O}$ value of all snow pits sampled during synoptic snow survey at maximum accumulation, (3) volume-weighted mean (VWM) of $\delta^{18}\text{O}$ of the snow lysimeter, and (4) time series of the snow lysimeter.

[31] Results from the various models were evaluated using two approaches. First, the uncertainty term W in equation (4) was parameterized by two means: (1) the standard deviation of the $\delta^{18}\text{O}$ values whenever the standard deviation could be defined with multiple samples and (2) using the analytical error of 0.05‰ from the $\delta^{18}\text{O}$ measurements at lab for components with a single sample. The term W was then weighted by multiplying the Student's t value at the confidence level of 95% so that the resultant

Table 1. Mean Percents of Two-Component Source Waters Separated From Discharge at the Martinelli and GL4 Catchments Using $\delta^{18}\text{O}$ Along With Uncertainties (1σ) at $\alpha = 0.05$ and Success Ratios (SR)^a

Code	New Water Parameterization	Martinelli				GL4			
		New, %	Old, %	Uncertainty	SR	New, %	Old, %	Uncertainty	SR
<i>Old Water Characterized by a Constant Base Flow</i>									
M1B	bulk value of the index snow pit at maximum accumulation	107	-7	7	7/18	40	60	2	18/18
M2B	mean of snow pits sampled at maximum accumulation	150	-50	220	4/18	47	53	24	18/18
M3B	original time series of snowmelt in snow lysimeter	149	-49	14	5/18	43	57	3	18/18
M4B	volume-weighted mean of snowmelt in snow lysimeter	92	8	89	8/18	38	62	16	18/18
M5B	date-stretched snowmelt in snow lysimeter	82	18	6	18/18	36	64	2	18/18
<i>Old Water Characterized by Time Series of Soil Water</i>									
M1S	bulk value of the index snow pit at maximum accumulation	106	-6	2	7/18	67	33	1	18/18
M2S	mean of snow pits sampled at maximum accumulation	120	-20	50	4/18	73	27	19	18/18
M3S	original time series of snowmelt in snow lysimeter	116	-16	3	5/18	70	30	1	18/18
M4S	volume-weighted mean of snowmelt in snow lysimeter	101	-1	36	8/18	65	35	16	18/18
M5S	date-stretched snowmelt in snow lysimeter	95	5	2	18/18	64	36	1	18/18

^aSee text for explanation on uncertainty and SR.

uncertainty was referred to as $\alpha = 0.05$ [Geneux, 1998]. Second, we evaluated for each time step whether the contribution of each component to streamflow had a reasonable range from 0 to 100%, and calculated the ratio of these successful solutions to the total number of stream samples (SR equals success ratio).

[32] Old water values differed depending on whether soil water or base flow was used to parameterize the old water component (Table 1). At the Martinelli catchment, the old water component ranged from 8% to -50% using base flow and from 5% to -20% using soil water, all arithmetically averaged from measured samples (hereinafter the same for all mean percentages). At the GL4 catchment, the old water component parameterized using base flow was about twice that of the old water contribution using soil water.

[33] The source water separations appeared to be even more sensitive to parameterization of new water (Table 1). Using the bulk $\delta^{18}\text{O}$ value of the index snow pit at maximum accumulation, for example, new water contributed 107% on average and old water contributed -7% if old water was parameterized by base flow at the Martinelli catchment. The SR value indicated that only 7 among 18 samples were successfully separated. Somewhat surprisingly, the separation became even worse when the original time series of $\delta^{18}\text{O}$ values in the snowmelt lysimeter was used, with a new water contribution of 149% and old water contribution of -49%. The SR value was only 5 of 18 samples and the uncertainty was 14%.

[34] The two-component modeling results were very different for the larger GL4 catchment (Table 1). All parameterizations of the new water provided reasonable contributions for all samples (SR = 18/18). Uncertainties for the GL4 catchment were much lower than the Martinelli catchment for all models. The proportion of new water varied from 36% to 47% using base flow to represent old water and from 64% to 73% using soil water to represent old water, with an uncertainty ranging from 1% to 24%.

[35] The primary reason for the poor model performance (negative values) at the Martinelli catchment was that the $\delta^{18}\text{O}$ values of snow and snowmelt were not always distinct from streamflow values due to their spatial and temporal variation (Figure 4a). We needed to develop a method to match the time frame of snowmelt at the snow lysimeter site

to that of discharge from the catchments. We developed a Monte Carlo procedure to randomly select 14 samples from streamflow at the Martinelli catchment and correlate with all 14 samples from the snow lysimeter for $\delta^{18}\text{O}$ content. In all runs the $\delta^{18}\text{O}$ values were kept in chronological order. The model was run for 10,000 iterations and the set with the highest correlation was selected ($r = +0.95$; $n = 14$). The dates from the streamflow were then used to substitute the dates for the $\delta^{18}\text{O}$ values of the snowmelt samples. Essentially the Monte Carlo simulations allowed us to stretch the time period that the samples were collected from the snowmelt lysimeter over the longer period of snowmelt runoff at the catchment.

[36] The date-stretched snowmelt values appeared to improve the two-component source water model at the Martinelli catchment (Table 1). The date-stretched snowmelt values suggest a new water component of 82% and an old water contribution of 18% for the model using base flow as old water, with an SR of 18/18 and an uncertainty of only 6%. At the larger Green Lake 4 catchment, however, the difference was relatively small in the new water component when comparing measured snowmelt values with the Monte Carlo results, with a change from 43% to 36% (Table 1). The error was similar from the two approaches at the Green Lake 4 catchment, which was less than 3%.

[37] A time series of separated hydrograph using base flow $\delta^{18}\text{O}$ for old water is shown in Figure 5. Daily values of new and old water fractions were linearly interpolated from results of measured samples (the same hereinafter for all daily interpolated flow components). For the Martinelli catchment, at all times discharge was composed almost entirely of new water. However, at the larger GL4 catchment, the amount of new water changed with time. During the rising limb and the high-flow period, discharge was composed of about 40% new water. After day 225, the new water component gradually decreased to near zero at base flow conditions.

4.5. Two-Component Mixing Model: Unreacted and Reacted Waters

[38] A two-component hydrograph separation was conducted to identify reacted and unreacted waters following the procedure of Sueker *et al.* [2000], who used concentrations

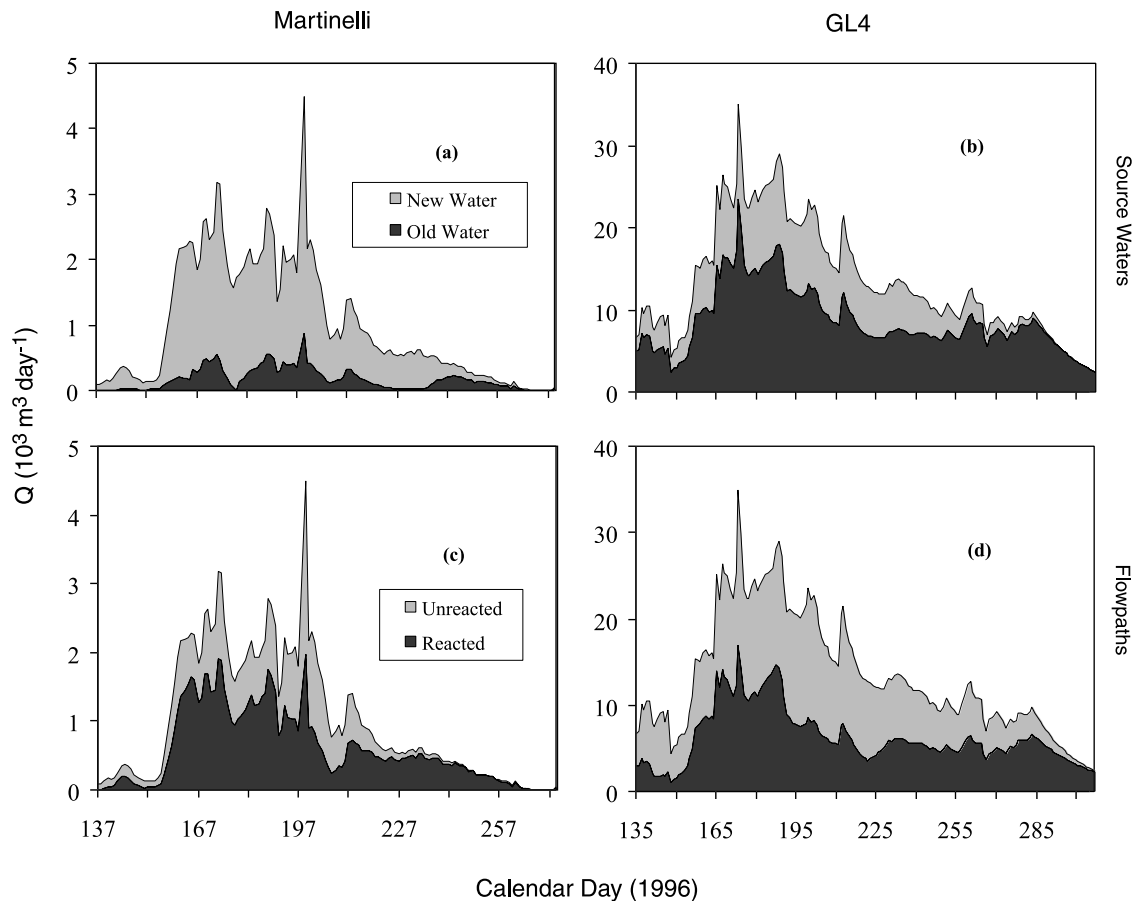


Figure 5. Results of two-component mixing models for source waters using $\delta^{18}\text{O}$ at (a) Martinelli and (b) GL4 catchment and for flow paths using Si at (c) Martinelli and (d) GL4 catchment. Daily discharge is linearly interpolated on the basis of the observed samples.

of Na^+ in snow and base flow for their flow path separation in stream waters of the Colorado Rocky Mountains. We used a similar approach and evaluated the use of five different tracers (Table 2): Na^+ , Si, ANC, Ca^{2+} , and SO_4^{2-} .

[39] At the Martinelli catchment, results using Si had the highest SR value at 18/18 and the lowest error at 6% (Table 2). The results using Si suggests an unreacted contribution of 39% and a reacted water contribution of 61%. Those results agree reasonably well with an earlier study [Caine, 1989], in which the recession limb of hydrograph including high-flow period was separated from 1984 to 1987. Hydrograph separation results at the GL4 catchment using Si suggest that unreacted water contributed 56% of streamflow and reacted

water 44% of streamflow. The use of Na^+ as a tracer at both catchments provides similar results but with higher error.

[40] A time series of the two-component hydrograph separation using Si suggests similar patterns in both catchments (Figures 5c and 5d). Reacted water provided half or more of streamflow on the rising limb of the hydrograph. Near peak discharge unreacted water was the major contribution to streamflow. About 30 days after peak discharge reacted water again became the dominant flow mechanism.

4.6. Three-Component Mixing Model: Flow Paths

[41] Three-component hydrograph separations were conducted using EMMA. Conservative tracers were evaluated

Table 2. Two-Component Separation of Discharge for Reacted and Unreacted Waters Using Geochemical Tracers at the Martinelli and GL4 Catchments in 1996^a

Geochemical Tracers	Martinelli				GL4, %			
	Unreacted, %	Reacted, %	Uncertainty	SR	Unreacted, %	Reacted, %	Uncertainty	SR
Na^+	33	67	13	17/18	60	40	16	18/18
Si	39	61	6	18/18	56	44	6	18/18
ANC	34	66	6	17/18	58	42	7	18/18
Ca^{2+}	20	80	6	15/18	47	53	5	18/18
SO_4^{2-}	15	85	11	14/18	61	39	3	18/18

^aReacted water is characterized by a base flow value, and unreacted water is characterized by the index snow pit data. Uncertainties and SR are calculated the same as in Table 1. Means are taken only from day 140 to 270, a period that is approximately identical with the source water separations in Table 1.

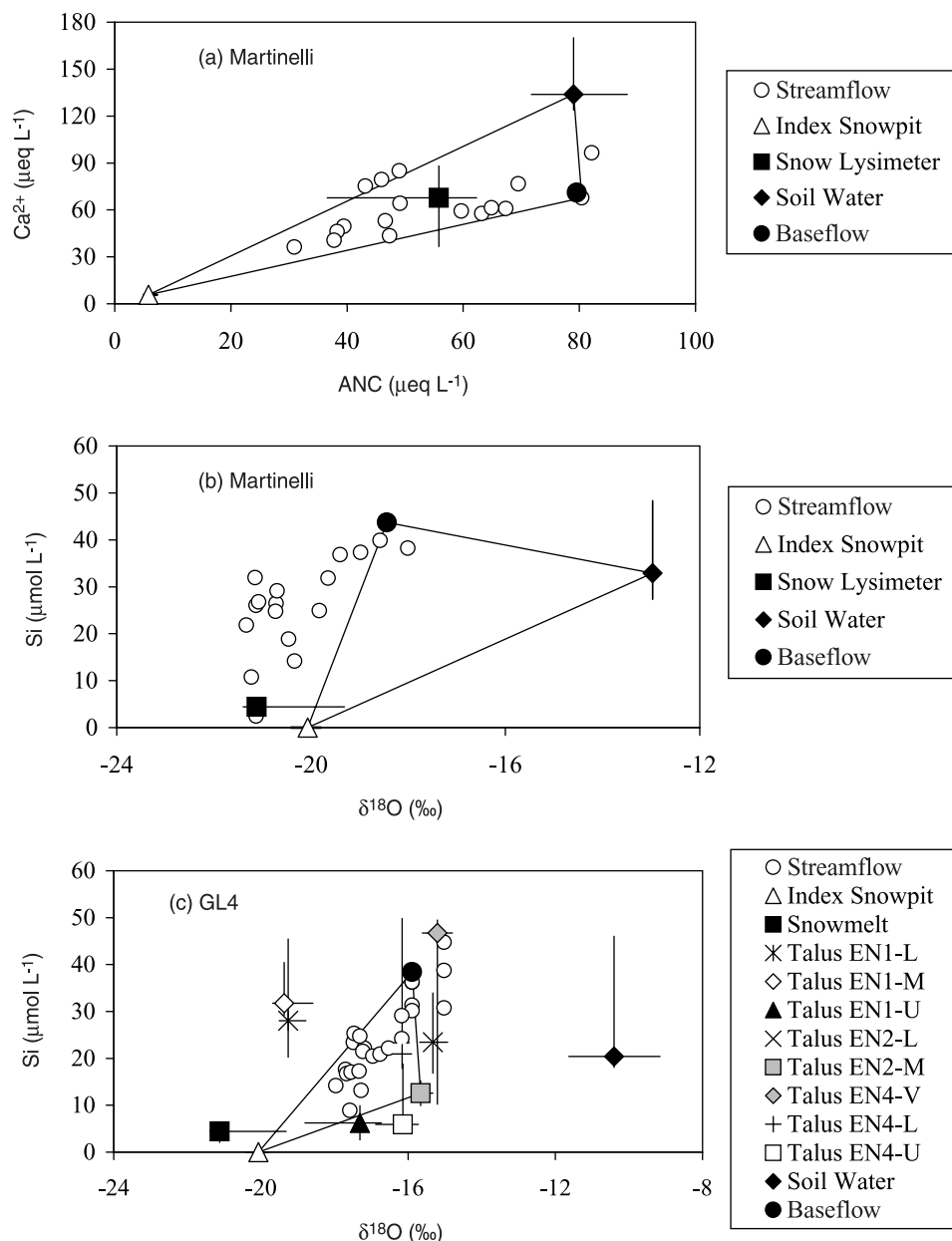


Figure 6. Conservative tracers evaluated by plotting medians and quartiles of potential end-members along with solute concentrations of stream flow. A total of 55 mixing diagrams were evaluated for each catchment. Here we show results from (a) the Martinelli catchment using ANC and Ca^{2+} , (b) the Martinelli catchment using $\delta^{18}\text{O}$ and Si, and (c) the GL4 catchment using Si and $\delta^{18}\text{O}$.

using mixing diagrams of *Christophersen et al.* [1990] and *Hooper et al.* [1990]. Tracer compositions of streamflow samples were plotted along with median and quartiles of potential end-members. Tracers were considered acceptable if streamflow samples were bounded by potential end-members, as demonstrated in Figure 6. A total of 55 mixing diagrams were evaluated for each catchment, including all potential combinations of paired tracers for Ca^{2+} , Mg^{2+} , Na^+ , K^+ , Cl^- , NO_3^- , SO_4^{2-} , ANC, Si, $\delta^{18}\text{O}$ and conductance. Eight tracers were found acceptable in each catchment: conductance, ANC, Ca^{2+} , Mg^{2+} , Na^+ , SO_4^{2-} , Si and $\delta^{18}\text{O}$.

[42] A principal component analysis (PCA) was performed using the correlation matrix of streamflow data to extract eigenvalues and eigenvectors. All eight tracers

mentioned above were used at the GL4 catchment, but $\delta^{18}\text{O}$ was not used at the Martinelli catchment because the mixing diagrams of $\delta^{18}\text{O}$ with chemical tracers cannot be well defined with available end-members (Figure 6b). The first two PCA components explain 92% of the total variance of the streamflow data at the Martinelli catchment and 91% at the GL4 catchment. On the basis of the work by *Christophersen and Hooper* [1992], three end-members appear to be sufficient to explain the total variance of solute and isotopic content of streamflow using EMMA.

[43] The streamflow data were standardized and projected onto U space defined by the eigenvector, along with all end-members (Figure 7). The same three end-members in the mixing diagram above also appear to be geometrically

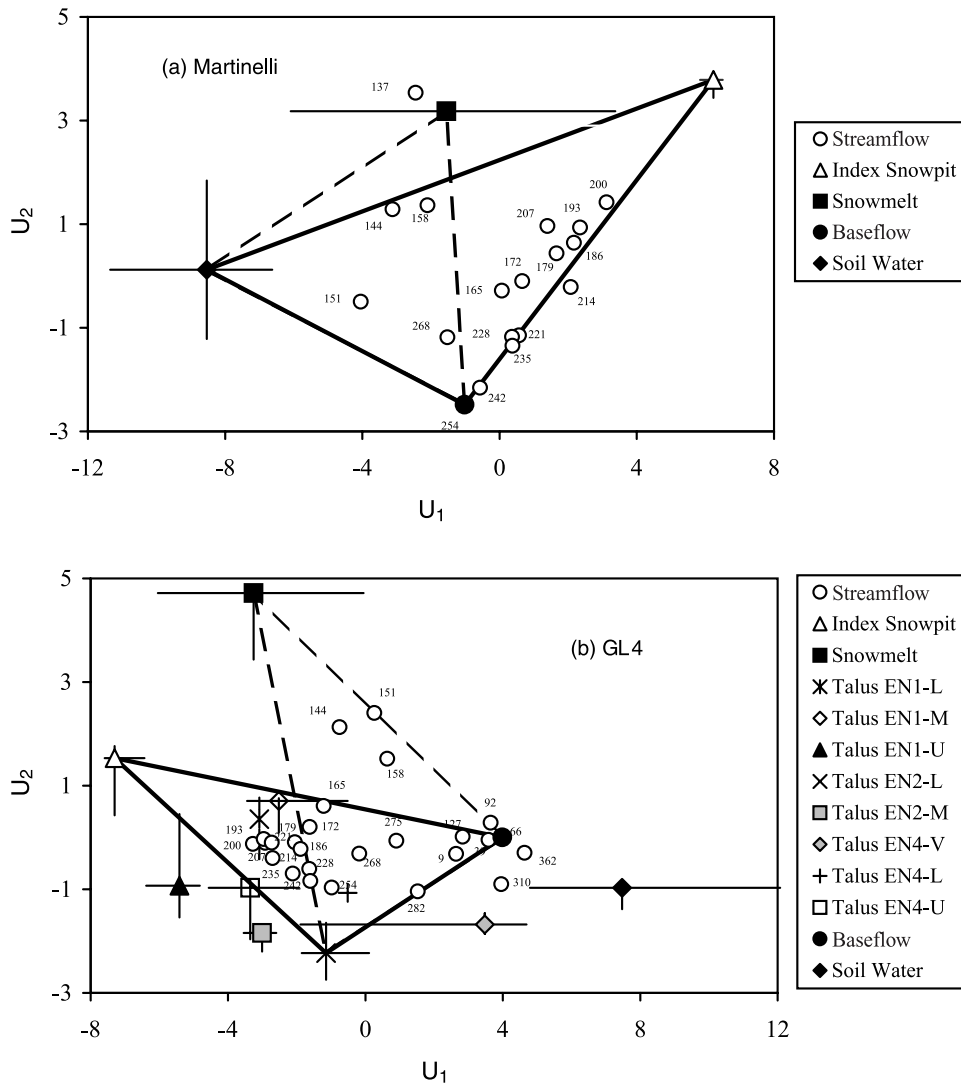


Figure 7. Orthogonal projections of end-members onto U space defined by stream water chemistry at (a) Martinelli catchment and (b) at Green Lake 4 catchment. End-members are shown by their medians and 25% and 75% quartiles. Numbers adjacent to samples are calendar day on which samples were collected. Triangle of dashed lines was used for samples on and around day 151 to account for ionic pulse.

correct in binding the streamflow samples for the Martinelli catchment and for the GL4 catchment except talus water. Talus water EN2-L appears to be better than EN2-M in binding the streamflow samples from a geometrical perspective. The Euclidean distance of end-member compositions between the U space and the S space was lower for talus water EN2-L than for EN2-M for all tracers except SO_4^{2-} (Table 3), demonstrating that talus water EN2-L is superior to EN2-M in EMMA. The distance was greater for some of the tracers in the index snow pit due to their low concentrations, with high values ranging from 60% to 260%. While these differences are relatively high, they are comparable to those reported by *Christophersen and Hooper* [1992]. Flow paths were determined using the first two U space projections. To account for the ionic pulse, samples collected at the initiation of snowmelt were resolved using snowmelt as an end-member, including sample on days 144 to 158 at both catchments (Figure 7).

[44] At the Martinelli catchment, streamflow was composed of, on average, 37% surface flow, 9% soil water, and 54% base flow (Figure 8a). The surface flow contribution was greater on the rising limb and during the high-flow period, with a relatively constant proportion of 40%. After the highest discharge peak on day 200, surface flow rapidly decreased. The soil water contribution was higher on the rising limb than the recession limb. Temporal variation in base flow showed a similar pattern as streamflow, with a gradual increase in proportion and decrease in discharge from the high-flow period in late spring to the end of snowmelt season.

[45] Surface flow at the GL4 catchment was almost identical with the Martinelli catchment at 36% of total discharge. However, base flow was much less than at the Martinelli catchment at 28%. Talus waters contributed 36%, the same amount as surface flow. Both maximum flow amount and percent of talus water contribution occurred on

Table 3. Difference of End-Members Between U Space Projections and Their Original Values (Medians) at the Martinelli and GL4 Catchments, 1996^a

End-Members	Conductance, %	ANC, %	Ca ²⁺ , %	Mg ²⁺ , %	Na ⁺ , %	SO ₄ ²⁻ , %	Si, ^b %	δ ¹⁸ O, %
<i>Martinelli Catchment</i>								
Index snow pit	-38	-156	75	153	-54	7	-	-
Snowmelt in lysimeter	9	-37	7	-26	70	48	47	-
Soil water	-2	15	-3	-28	9	59	-42	-
Base flow	1	1	2	-2	2	-7	-6	-
<i>Green Lake 4 Catchment</i>								
Index snow pit	-17	-118	139	203	-260	-131	-	-3
Snowmelt in lysimeter	21	-66	4	-6	32	78	-168	-5
Talus EN1-L	39	-38	6	-1	-36	130	-48	-8
Talus EN1-M	22	-38	8	-11	-17	193	-53	-8
Talus EN1-U	-13	35	6	-13	-20	11	85	3
Talus EN2-L	-10	38	2	-26	-16	86	19	5
Talus EN2-M	-22	65	-2	-26	18	34	67	7
Talus EN4-V	-2	0	-16	-10	59	20	-16	-1
Talus EN4-L	0	-32	-10	-6	38	45	22	2
Talus EN4-U	-17	3	2	-22	77	19	184	7
Soil water	-48	146	24	-10	66	65	114	43
Base flow	0	-3	6	-3	14	-9	3	1

^aDifference is normalized to percentage by dividing by their original value.

^bPercentage cannot be calculated for the index snow pit in that the median of its original concentration is zero.

the recession limb of the hydrograph (Figure 8b). In August and September (day 210 to 255), talus waters contributed more than 50% of total discharge. Somewhat counterintuitively, base flow attained its highest discharge in the spring runoff season. During summer and early fall, base flow kept a constant discharge. The proportion of surface flow was highest at the beginning of snowmelt and gradually decreased as snowmelt progressed.

[46] The EMMA solutions were evaluated by reproducing concentrations of all conservative tracers from the EMMA model and comparing them to the measured values. For the Martinelli catchment, EMMA slightly underpredicted the observed arithmetic mean value for Ca²⁺, Na⁺, and SO₄²⁻ and overpredicted for conductance, ANC, and Mg²⁺ (Table 4). The Pearson correlation coefficient was greater than 0.9 for all solutes except SO₄²⁻ at 0.85 and Si at 0.8. At the GL4 catchment, results were somewhat better compared to the Martinelli catchment. The difference of means was less than 5% for all solutes except SO₄²⁻ at -9%. Pearson correlations were all greater than 0.9, except for ANC at 0.8.

5. Discussion

5.1. Source Waters

[47] Our results show that systematic errors in hydrograph separation may be introduced if the temporal variation in δ¹⁸O of meltwater is ignored and the average value of the δ¹⁸O of the snowpack is used as the new water composition. Taylor *et al.* [2002] have suggested that the magnitude of this error is proportional to the new water fraction and to the isotopic difference between the average snowpack value and meltwater, and is inversely proportional to the isotopic differences between the old water and the average snowpack value. Our results are consistent with the report of Taylor *et al.* [2001, 2002].

[48] An outstanding question is how to incorporate changes in the isotopic composition of meltwater measured at a point into distributed models for hydrograph separation. The temporal enrichment of the δ¹⁸O values in snowmelt is

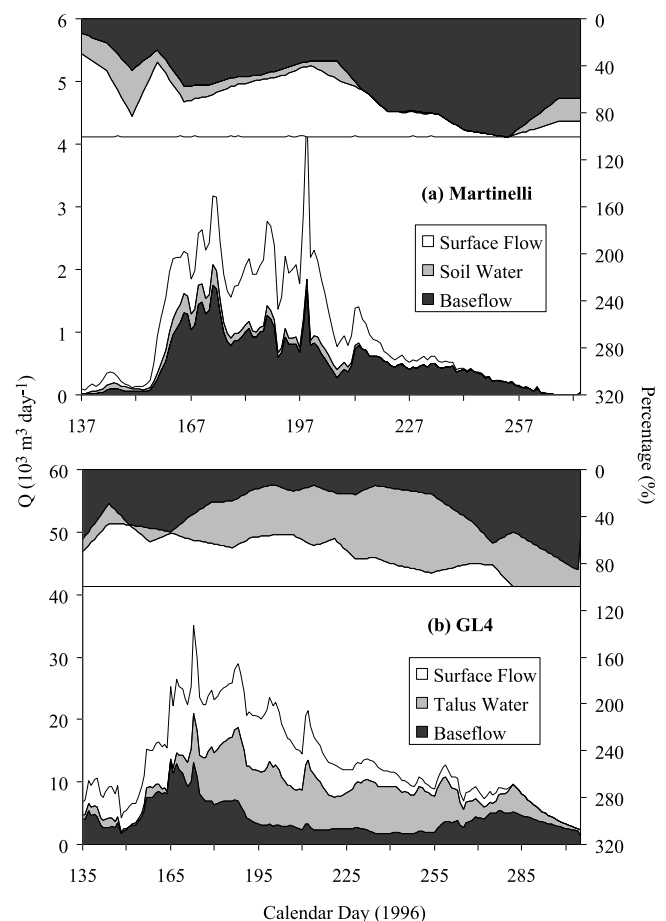


Figure 8. Time series of three-component mixing models using EMMA for (a) Martinelli and (b) Green Lake 4 catchment. Daily discharge is linearly interpolated based on the observed samples.

Table 4. Comparison of Observed and Predicted Tracer Concentrations Using the EMMA Results at the Martinelli and GL4 Catchments, 1996^a

	Conductance	ANC	Ca ²⁺	Mg ²⁺	Na ⁺	SO ₄ ²⁻	Si	δ ¹⁸ O
<i>Martinelli Catchment (n = 18)</i>								
Observed Mean	9.6	55.2	62.4	10.0	15.8	15.9	27.0	
Predicted Mean	9.8	58.7	60.6	10.9	15.1	14.3	27.2	
Difference	1	3	-2	4	-2	-5	0	
Pearson Coefficient	0.98	0.90	0.99	0.98	0.91	0.85	0.80	
<i>Green Lake 4 Catchment (n = 26)</i>								
Observed Mean	12.3	46.6	74.5	14.6	15.6	41.6	24.9	-16.7
Predicted Mean	12.7	50.1	72.2	14.3	17.8	34.9	25.0	-16.8
Difference	2	4	-2	-1	5	-9	0	1
Pearson Coefficient	0.98	0.80	0.98	0.97	0.94	0.94	0.92	0.90

^aUnits for mean concentrations are the same as in Figures 2 and 4. Difference (%) between observed and predicted means is normalized by dividing the sum of observed and predicted means.

a result of depletion of δ¹⁸O in the liquid water due to isotopic fractionation between the liquid phase and solid phase [Maule and Stein, 1990; Taylor et al., 2001, 2002]. We investigated whether the changes in the δ¹⁸O content of meltwater were dependent on the amount of melt. We regressed the δ¹⁸O values of snowmelt against the cumulative melted fraction of snow (*f*), where 1 - *f* is the fraction of the snowpack that has not melted. Simple linear regression shows that the δ¹⁸O content of meltwater was significantly correlated with the cumulative amount of snowmelt (*n* = 15, R² = 0.87, *p* < 0.001). As a result, the δ¹⁸O values in snowmelt measured at the point cannot be directly used for hydrograph separation in the catchment. The Monte Carlo procedure appears to work reasonably well to adapt the snowmelt δ¹⁸O values sampled at a point to the catchment scale.

[49] New water dominance at the Martinelli catchment may be due to the catchment's responsive behavior as a result of shallow soils and steep slopes [Caine, 1989]. Additionally, it may be caused by deep and long-lasting snow accumulation in the center of the basin. Buttle [1994] recognized that new water component tends to increase for snow-dominated catchments. McNamara et al. [1997] demonstrated that streamflow is nearly all new water during snowmelt period in Arctic regions with frozen soil. Williams et al. [1993] showed that preevent water at the Emerald Lake Watershed contributes only a small fraction of streamflow during the period of snowmelt runoff.

[50] The old water component at the GL4 catchment of 64 ± 2% that we report is higher than reports from neighboring watersheds in the Rocky Mountains. Mast et al. [1995] reported that old water accounts for 17% in Andrews Creek watershed in the Colorado Front Range. Sueker et al. [2000] also reported that new water is slightly greater than 50% in four of six alpine/subalpine basins in Colorado Rocky Mountain National Park. In their studies, old water is likely underestimated due to use of VWM δ¹⁸O in snowmelt [Mast et al., 1995] and a constant δ¹⁸O value in snowpack [Sueker et al., 2000]. The difference of δ¹⁸O between base flow (-16.7‰) and snowmelt (-19‰) at the Andrews Creek watershed is much smaller than that at the GL4 catchment. As a result, the underestimation of old water should be significant at the Andrews Creek watershed. Sueker et al. [2000] used a value of -19.5‰ to represent new water, which was calibrated based on Mast et

al. [1995] from a mean value of -20.43‰ from 14 snow pits sampled in mid-April. Their sensitivity analysis also shows that new water contributions to streamflow decrease by up to 5% for the entire study period when new water δ¹⁸O changes to -20‰. On the other hand, the old water in our case may be overestimated by ignoring rainfall, which has a δ¹⁸O signature even more enriched than soil water (Figure 4). Sueker et al. [2000] estimated that direct rain runoff accounts for 4–13% from May to October of 1994 with a rainfall/precipitation ratio greater than 25%. Because our rainfall/precipitation ratio is about 15%, however, the overestimation of old water may be insignificant.

5.2. Flow Path Models

[51] Unreacted water determined by Si (39 ± 6%) is about half of new water (82 ± 6%) at the Martinelli catchment. Old water (18 ± 6%) is also much less than subsurface flow from EMMA (soil water + base flow = 63%). Subsurface flow apparently contains new water, as reported by Wels et al. [1991a, 1991b] and Uhlenbrook and Hoeg [2003]. It appears that there should be a new end-member, subsurface event water. Subsurface event water may have the same δ¹⁸O signature as snowmelt, but its chemical composition may lie between new water and old water, on the basis of work by Buttle and Peters [1997]. This new end-member is also inferred from the mixing diagram of δ¹⁸O and Si (Figure 6b). Three end-members, snowmelt (the index snow pit), soil water and base flow, do not bound all the streamflow samples. However, if an end-member with the same δ¹⁸O value as snowmelt and Si concentration as base flow were used to substitute for soil water, all streamflow samples would be well bounded. The lack of this end-member may be the primary reason why Si and SO₄²⁻ concentrations in the streamflow were not well recreated by the EMMA results. Improvement of this EMMA model therefore necessitates field measurement of this end-member in the future.

[52] The old water component (64%) from the source water model using base flow for old water parameterization is identical with subsurface flow (talus flow + base flow = 64%) from the EMMA at the GL4 catchment (Figures 5b and 8b). The correlation coefficient between subsurface flow and old water is 0.65 (*n* = 18, *p* < 0.01). Since talus water is old water based on the δ¹⁸O signature (Figure 6c), agreement between subsurface flow and old water indicates that subsurface event water is insignificant at the GL4

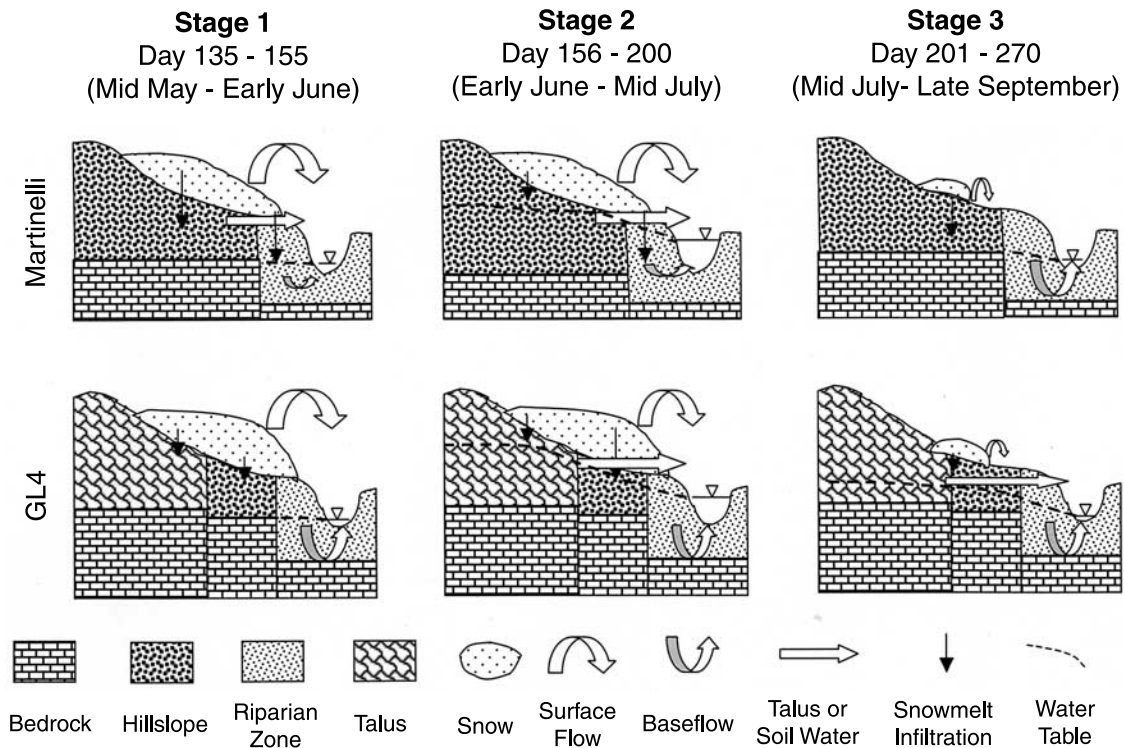


Figure 9. A sketch diagram illustrating flow generation at the Martinelli and GL4 catchments. Note that physical objects are not to scale, but size of block arrows represents relative importance of flow paths. Where a block arrow is not presented, the flow path it represents is near zero. Also, block arrows represent flow direction but not true flow tracks for the sake of clearness of the diagram.

catchment compared to the Martinelli catchment. It is also demonstrated that using base flow to parameterize old water for the source water model is reliable. Unlike $\delta^{18}\text{O}$, however, geochemical composition in talus water is distinct from base flow (Figure 6). Using geochemical tracer to partition unreacted and reacted water, two different reacted waters must be considered. If base flow is arbitrarily used to represent reacted water in two-component models, unreacted water is overestimated since the geochemical composition in base flow is much higher than in talus water. This is why unreacted water is greater than new water at the GL4 catchment (Tables 1 and 2). This may also explain why unreacted water is greater at the GL4 catchment than at the Martinelli catchment.

5.3. Conceptual Model of Source Waters and Flow Paths

[53] The hydrograph at both Martinelli and GL4 catchments suggests three distinct stages (Figure 9). Stage 1 is from the initiation of snowmelt to about day 155 (mid-May to early June), during which snowmelt is initiated and streamflow discharge is low (Figures 8a and 8b). Stage 2 is from day 156 to 200 (early June to mid-July), including a steeply rising limb in late spring to maximum discharge in early summer. Stage 3 spans from day 201 to about 270 (mid-July to late September), representing the main recession limb of hydrograph.

5.3.1. Martinelli Catchment

5.3.1.1. Stage 1

[54] Snowmelt occurs primarily in the near-channel portion of the lower watershed, where snowpack is relatively

shallow. A portion of the first fraction of meltwater from the snowpack infiltrates soils and unconsolidated materials (Figure 9). The infiltrating snowmelt increases soil moistures and undergoes rapid kinetic reactions with subsurface materials [Williams *et al.*, 1993; Mast *et al.*, 1995; Campbell *et al.*, 1995; Sueker *et al.*, 2000]. Additionally, a portion of this snowmelt appears to flow directly into the stream channel, consistent with results of Campbell *et al.* [2002]. Solute concentrations in the stream channel increase in part because of the release of solutes from the seasonal snowpack in the form of an ionic pulse. The ionic pulse, in combination with low discharge, may explain why solute concentrations in streamflow are relatively high (Figure 2) when new water component contributes near 100% during this stage (Figure 5a).

5.3.1.2. Stage 2

[55] Snowmelt dramatically intensifies and streamflow discharge rapidly increases (Figure 2c). Soils become saturated and saturation-excess overland flow occurs near the stream channels [Williams *et al.*, 1993]. Depression of solute concentration in this stage (Figure 2) may be a result of dilution of solute contents in subsurface flow (50–60%) by surface flow (40–50%) (Figure 8a). Complicating this interpretation is the potential role of seasonally frozen ground. The presence of seasonally frozen ground below the snow cover may reduce infiltration and facilitate surface flow. The potential role of seasonally frozen ground in the hydrology of high mountain catchments of the Colorado Front Range deserves more research [Clow *et al.*, 2003].

[56] Subsurface event water primarily occurs during this stage (Figures 5a and 8a). Delivery of subsurface event

water may be rapid [Wels *et al.*, 1991a, 1991b; Brown *et al.*, 1999], probably within an hour at the Martinelli catchment [Caine, 1989]. This water may be routed directly to the stream channels in the form of lateral flow as a thin saturated layer above the saturated zone [Wels *et al.*, 1991a, 1991b; Brown *et al.*, 1999]. This water can also reach to bedrock and soil interface via vertical preferential pathways [Buttle and McDonnell, 2002], mix with old water in vadose zone and saturated zone [Buttle, 1994], and rapidly travel to stream channel with old water [McDonnell, 1990]. It is unclear at this time whether preferential pathways exist at the Martinelli catchment. To confirm which mechanism predominates, hydrograph separation alone appears to be insufficient [Buttle and Peters, 1997] and physical measurements may be needed in the future.

5.3.1.3. Stage 3

[57] Streamflow behaves in a typical recession pattern. A mixture of new water and old water dominates the first 30 days after which old water dominates at base flow conditions (Figure 5a). Base flow is assumed to be primarily released from the storage in fractured bedrock (Figure 9).

5.3.2. GL4 Catchment

5.3.2.1. Stage 1

[58] Similar to the Martinelli catchment, meltwater may primarily infiltrate the ground during this stage (Figure 9). Different from the Martinelli catchment, soil water on hillslopes does not appear to contribute to streamflow. Base flow and old water may be primarily from fractured bedrock.

5.3.2.2. Stage 2

[59] Surface flow accounts for approximately 40% of streamflow (Figure 8b). Solute contents in subsurface flow are diluted by surface flow, resulting in depression of solute contents in streamflow (Figure 2). Water bodies occupy only 4% of the basin area [Meixner *et al.*, 2000]. Direct melt on lake and stream surface is insufficient to account for surface flow. Surface flow may occur primarily in the form of saturation-excess overland flow on soils near lakes and between lake 4 and lake 5 (Figure 1). As snowmelt rate increases, saturated areas in soils may expand and thus surface flow increases.

[60] Base flow peaks during the high-flow period at the GL4 catchment (Figure 7d), along with old water (Figure 5b). Subsurface flow matches old water in magnitude and in temporal pattern. Old water appears to be delivered via translatory flow, which is stored in the groundwater reservoir and released via a lateral through flow by a process of displacement by new water inputs [Hewlett and Hibbert, 1967; Buttle, 1994; McGlynn *et al.*, 2002]. Sklash *et al.* [1986] indicates that translatory flow in the near-stream zone is considered to be responsible for the large (>75%) contribution of preevent water to storm flow from the Maimai catchment in New Zealand. McDonnell *et al.* [1991] provide further evidence through tensiometric measurements that the near-stream zone is often close to or at saturation.

[61] Talus water is also a major contributor to the streamflow during this stage (Figure 7d). Burns *et al.* [2001] show that runoff from an outcrop of the forested Panola Mountain Research Watershed contributes more than 50% of the peak storm flow during two rainstorms. Similar to their results, our results demonstrate that the unique geographical setting of talus fields is important in controlling streamflow quantity and quality.

5.3.2.3. Stage 3

[62] Talus water continues to contribute to streamflow with an increasing proportion and relatively invariant discharge (Figure 8b). Discharge from base flow is also invariant, but with a much lower discharge than talus flow. At the end of the stage, base flow from fractured bedrock dominates the streamflow.

6. Conclusions

[63] Hydrograph separations for source waters are complicated by the temporal enrichment of $\delta^{18}\text{O}$ in snowmelt. First, ignorance of the variation may result in a significant underestimation of old water. Second, $\delta^{18}\text{O}$ values in snowmelt measured at a point should be adapted to the snowmelt regime at the catchment scale. With increasing catchment size, however, the sensitivity of source water separations to the enrichment may become dampened. Using geochemical tracers for unreacted and reacted waters in two-component models, the results were not always meaningful owing to violation of the mixing model assumptions. Also, source water models alone cannot explain flow pathways. EMMA using both isotopic and geochemical tracers indicates that subsurface flow contributes near or more than 60% of streamflow discharge even during the early snowmelt season when snowmelt and streamflow discharge attain their peaks. Soil water doesn't appear to be a significant contributor of streamflow in those high-elevation catchments. The large amount of subsurface flow (old water as well) at the GL4 catchment is due to talus water. The large contribution of talus water to streamflow confirms the speculation by Williams *et al.* [1997], Campbell *et al.* [1995], and Meixner *et al.* [2000] that NO_3^- in talus fields may contribute to stream waters of high-elevation catchments in the Colorado Front Range. The large amount of groundwater was not expected. These results strongly suggest that surface water and groundwater interactions are much more important to the quantity and quality of surface water in high-elevation catchments than previously thought.

Appendix A

[64] Figure A1 shows an example for solving outliers in a three end-member model. A, B, and C are three end-members. Streamflow sample D is an outlier, just outside the triangle confined by the end-members and on the side of line AB. E is the projection of D on the line AB. Small case characters *a*, *b*, and *d* represent distances of D and A, D and B, and A and B. Given that the coordinates of A, B, and D are expressed by (A_{U1}, A_{U2}) , (B_{U1}, B_{U2}) , and (D_{U1}, D_{U2}) , values of *a*, *b* and *d* can be simply determined using Pythagorean theorem:

$$a = \sqrt{(A_{U1} - D_{U1})^2 + (A_{U2} - D_{U2})^2} \quad (\text{A1})$$

$$b = \sqrt{(B_{U1} - D_{U1})^2 + (B_{U2} - D_{U2})^2} \quad (\text{A2})$$

$$d = \sqrt{(B_{U1} - A_{U1})^2 + (B_{U2} - A_{U2})^2} \quad (\text{A3})$$

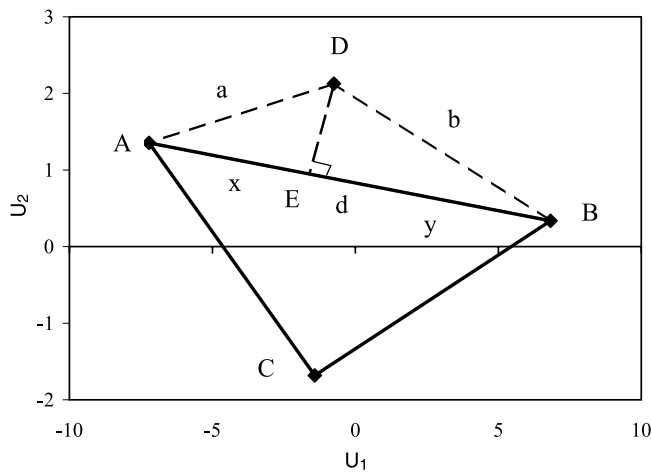


Figure A1. Diagram illustrating how an outlier is resolved using a geometrical approach.

Similarly, x and y can be solved by Pythagorean theorem and expressed as a function of a , b and d :

$$x = \frac{a^2 + d^2 - b^2}{2d^2} \quad (\text{A4})$$

$$y = 1 - x \quad (\text{A5})$$

Note that x is normalized by dividing x by d in equation (A4) to convert x into fraction and thus y is just equal to 1 minus x .

[65] Contribution of the end-member C to sample D is assumed to be zero [Christophersen and Hooper, 1992]. Fractions of end-members A and B (f_A and f_B) are inversely proportional to their distance to E, namely,

$$\frac{f_A}{f_B} = \frac{y}{x} \quad (\text{A6})$$

Note that $f_A + f_B = 1$. If equations (A4) and (A5) are brought into equation (A6), then,

$$f_A = y \quad (\text{A7})$$

$$f_B = x \quad (\text{A8})$$

Remember that equations (A7) and (A8) only apply to the situation that D's projection lies between A and B. If the projection is beyond A or B, then it is assumed that $f_B = 0$ and $f_A = 1$ or $f_A = 0$ and $f_B = 1$. This is the situation when two end-member solutions are negative in a three end-member EMMA model.

[66] **Acknowledgments.** T. Bardsley, C. Seibold, and Oliver Platts-Mills provided field and laboratory assistance. Funding assistance was provided by National Science Foundation grants DEB 9211776 and DEB 9810218 to the NWT LTER site, by the NSF Division of Environmental Geochemistry and Biogeochemistry, by the Air Resources Division of the National Park Service, and NASA EOS grant NAGW-2602.

References

- Baron, J. S., D. S. Ojima, E. A. Holland, and W. J. Parton (1994), Analysis of nitrogen saturation potential in Rocky Mountain tundra and forest: Implication for aquatic system, *Biogeochemistry*, 27, 61–82.
- Baron, J. S., H. M. Rueth, A. M. Wolfe, K. R. Nydick, E. J. Allstott, J. T. Minear, and B. Moraska (2000), Ecosystem responses to nitrogen deposition in the Colorado Front Range, *Ecosystems*, 3, 352–368.
- Bottomley, D. J., D. Craig, and L. M. Johnston (1986), Oxygen-18 studies of snowmelt runoff in a small Precambrian Shield watershed: Implications for streamwater acidification in acid-sensitive terrain, *J. Hydrol.*, 88, 213–234.
- Brown, V. A., J. J. McDonnell, D. A. Burns, and C. Kendall (1999), The role of event water, a rapid shallow flow component, and catchment size in summer stormflow, *J. Hydrol.*, 217, 171–190.
- Burns, D. A. (2002), The effects of atmospheric nitrogen deposition in the Rocky Mountains of Colorado and southern Wyoming—A synthesis and critical assessment of published results, *U.S. Geol. Surv. Water Resour. Invest. Rep.*, 02-4066.
- Burns, D. A., J. J. McDonnell, R. P. Hooper, N. E. Peters, J. E. Freer, C. Kendall, and K. Beven (2001), Quantifying contributions to storm runoff through end-member mixing analysis and hydrologic measurements at the Panola Mountain Research Watershed (Georgia, USA), *Hydrol. Processes*, 15(10), 1903–1924.
- Buttle, J. M. (1994), Isotope hydrograph separations and rapid delivery of pre-event water from drainage basins, *Prog. Phys. Geogr.*, 18, 16–41.
- Buttle, J. M., and J. J. McDonnell (2002), Coupled vertical and lateral preferential flow on a forested slope, *Water Resour. Res.*, 38(5), 1060, doi:10.1029/2001WR000773.
- Buttle, J. M., and D. L. Peters (1997), Inferring hydrological process in a temperate basin using isotopic and geochemical hydrograph separation: A re-evaluation, *Hydrol. Processes*, 11, 557–573.
- Caine, N. (1989), Hydrograph separation in a small alpine basin based on inorganic solute concentrations, *J. Hydrol.*, 112, 89–101.
- Caine, N., and E. M. Thurman (1990), Temporal and spatial variations in solute content of an alpine stream, Colorado Front Range, *Geomorphology*, 4, 55–72.
- Campbell, D. H., D. W. Clow, G. P. Ingersoll, M. A. Mast, N. E. Spahr, and J. T. Turk (1995), Processes controlling the chemistry of two snowmelt-dominated streams in the Rocky Mountains, *Water Resour. Res.*, 31(11), 2811–2821.
- Campbell, D. H., C. Kendall, C. C. Y. Chang, S. R. Silva, and K. A. Tonnesen (2002), Pathways for nitrate release from an alpine watershed: Determination using $\delta^{15}\text{N}$ and $\delta^{18}\text{O}$, *Water Resour. Res.*, 38(5), 1052, doi:10.1029/2001WR000294.
- Christophersen, N., and R. P. Hooper (1992), Multivariate analysis of stream water chemical data: The use of principal components analysis for the end-member mixing problem, *Water Resour. Res.*, 28(1), 99–107.
- Christophersen, N., C. Neal, R. P. Hooper, R. D. Vogt, and S. Andersen (1990), Modeling stream water chemistry as a mixture of soil water end-members—A step towards second-generation acidification models, *J. Hydrol.*, 116, 307–320.
- Cirno, C. P., and J. J. McDonnell (1997), Linking the hydrologic and biogeochemical controls of nitrogen transport in near-stream zones of temperate-forested catchments: A review, *J. Hydrol.*, 199, 88–120.
- Clow, D., L. Schrott, R. Webb, D. H. Campbell, A. Torizzo, and M. Domblaser (2003), Ground water occurrence and contributions to streamflow in an alpine catchment, Colorado Front Range, *Ground Water*, 41(7), 937–950.
- Genereux, D. P. (1998), Quantifying uncertainty in tracer-based hydrograph separations, *Water Resour. Res.*, 34(4), 915–919.
- Hewlett, J. D., and A. R. Hibbert (1967), Factors affecting the response of small watersheds to precipitation in humid areas, in *Forest Hydrology*, edited by W. E. Sopper and H. W. Lull, pp. 275–290, Pergamon, New York.
- Holko, L., and A. Lepisto (1997), Modelling the hydrological behavior of a mountain catchment using TOPMODEL, *J. Hydrol.*, 196, 361–377.
- Hooper, R. P. (2003), Diagnostic tools for mixing models of stream water chemistry, *Water Resour. Res.*, 39(3), 1055, doi:10.1029/2002WR001528.
- Hooper, R. P., and C. A. Shoemaker (1986), A comparison of chemical and isotopic hydrograph separation, *Water Resour. Res.*, 22(10), 1444–1454.
- Hooper, R. P., N. Christophersen, and N. E. Peters (1990), Modeling stream water chemistry as a mixture of soil water end-members—An application to the Panola mountain catchment, Georgia, U.S.A., *J. Hydrol.*, 116, 321–343.
- Ingrahan, N. L., and B. E. Taylor (1989), The effect of snowmelt on the hydrogen isotope ratios of creek discharge in Surprise Valley, California, *J. Hydrol.*, 106, 233–244.
- Joerin, C., K. J. Beven, I. Iorgulescu, and A. Musy (2002), Uncertainty in hydrograph separations based on geochemical mixing models, *J. Hydrol.*, 255, 90–106.

- Laudon, H., H. F. Hemond, R. Krouse, and K. H. Bishop (2002), Oxygen 18 fractionation during snowmelt: Implication for spring flood hydrograph separation, *Water Resour. Res.*, 38(11), 1258, doi:10.1029/2002WR001510.
- Litaor, M. I. (1993), The influence of soil interstitial waters on the physicochemistry of major, minor and trace metals in stream waters of the Green Lakes Valley, Front Range, Colorado, *Earth Surf. Processes Landforms*, 18, 489–504.
- Mast, M. A., C. Kendall, D. H. Campbell, D. W. Clow, and J. Back (1995), Determination of hydrologic pathways in an alpine-subalpine basin using isotopic and chemical tracers, Loch Vale Watershed, Colorado, USA, in *Biogeochemistry of Seasonally Snow-Covered Catchments (Proceedings of a Boulder Symposium, July 1995)*, edited by K. A. Tonnessen, M. W. Williams, and M. Tranter, *IAHS Publ.*, 228, 263–270.
- Maule, C. P., and J. Stein (1990), Hydrologic flow path definition and partitioning of spring meltwater, *Water Resour. Res.*, 26(12), 2959–2970.
- McDonnell, J. J. (1990), A rationale for old water discharge through macropores in a steep, humid catchment, *Water Resour. Res.*, 26(11), 2821–2832.
- McDonnell, J. J., I. F. Owens, and M. K. Steward (1991), A case study of shallow flow paths in a steep zero-order basin: A physical-chemical-isotopic analysis, *Water Resour. Bull.*, 27, 679–685.
- McGlynn, B. L., J. J. McDonnell, and D. D. Brammer (2002), A review of the evolving perceptual model of hillslope flowpaths at the Maimai catchments, New Zealand, *J. Hydrol.*, 257, 1–26.
- McNamara, J. P., D. L. Kane, and L. D. Hinzman (1997), Hydrograph separations in an Arctic watershed using mixing model and graphical techniques, *Water Resour. Res.*, 33(7), 1707–1719.
- Meixner, T., R. C. Bales, M. W. Williams, D. H. Campbell, and J. S. Baron (2000), Stream chemistry modeling of two watersheds in the Front Range, Colorado, *Water Resour. Res.*, 36(1), 77–87.
- Neal, C. (2001), Alkalinity measurements within natural waters: Towards a standardised approach, *Sci. Total Environ.*, 265, 99–113.
- Perakis, S. S. (2002), Nutrient limitation, hydrology and watershed nitrogen loss, *Hydrol. Processes*, 16, 3507–3511.
- Rodhe, A. (1981), Spring flood: Meltwater or groundwater?, *Nord. Hydrol.*, 12, 21–30.
- Rodhe, A. (1987), The origin of streamwater traced by oxygen-18, *Rep. Ser. A41*, 260 pp., Dep. of Phys. Geogr., Uppsala Univ., Uppsala, Sweden.
- Sklash, M. G., R. N. Farvolden, and P. Fritz (1976), A conceptual model of watershed response to rainfall, developed through the use of oxygen-18 as a natural tracer, *Can. J. Earth Sci.*, 13, 271–283.
- Sklash, M. G., M. K. Steward, and A. J. Pearce (1986), Storm runoff generation in humid headwater catchments: 2. A case study of hillslope and low-order stream response, *Water Resour. Res.*, 22, 1273–1282.
- Soulsby, C., J. Petry, M. J. Brewer, S. M. Dunn, B. Ott, and I. A. Malcolm (2003), Identifying and assessing uncertainty in hydrological pathways: A novel approach to end-member mixing in a Scottish agricultural catchment, *J. Hydrol.*, 274, 109–128.
- Sueker, J., J. N. Ryan, C. Kendall, and R. D. Jarrett (2000), Determination of hydrologic pathways during snowmelt for alpine/subalpine basins, Rocky Mountain National Park, Colorado, *Water Resour. Res.*, 36(1), 63–75.
- Taylor, S., X. Feng, J. W. Kirchner, R. Osterhuber, B. Klauke, and C. E. Renshaw (2001), Isotopic evolution of a seasonal snowpack and its melt, *Water Resour. Res.*, 37(3), 759–769.
- Taylor, S., X. Feng, M. Williams, and J. McNamara (2002), How isotopic fractionation of snowmelt affects hydrograph separation, *Hydrol. Processes*, 16, 3683–3690.
- Uhlenbrook, S., and S. Hoeg (2003), Quantifying uncertainties in tracer-based hydrograph separations: A case study for two-, three- and five-component hydrograph separations in a mountainous catchment, *Hydrol. Processes*, 17, 431–453.
- Unnikrishna, P. V., J. J. McDonnell, and C. Kendall (2002), Isotope variations in a Sierra Nevada snowpack and their relation to meltwater, *J. Hydrol.*, 260, 38–57.
- Wels, C., B. J. Cornett, and B. D. LaZerte (1990), Groundwater and wetland contributions to stream acidification: An isotopic analysis, *Water Resour. Res.*, 26(12), 2993–3003.
- Wels, C., R. J. Cornett, and B. D. LaZerte (1991a), Hydrograph separation: A comparison of geochemical and isotopic tracers, *J. Hydrol.*, 122, 253–274.
- Wels, C., C. H. Taylor, R. J. Cornett, and B. D. LaZerte (1991b), Stream flow generation in a headwater basin on the Precambrian Shield, *Hydrol. Processes*, 5, 185–199.
- Williams, M. W., and N. Caine (2002), Hydrology and hydrochemistry, in *Alpine Dynamics: The Structure and Function of an Alpine Ecosystem: Niwot Ridge, Colorado*, edited by W. Bowman and T. R. Seastedt, pp. 75–98, Oxford Univ. Press, New York.
- Williams, M. W., and K. A. Tonnessen (2000), Critical loads for inorganic nitrogen deposition in the Colorado Front Range, USA, *Ecol. Appl.*, 10(6), 1648–1665.
- Williams, M. W., A. D. Brown, and J. M. Melack (1993), Geochemical and hydrologic controls on the composition of surface water in a high-elevation basin, Sierra Nevada, California, *Limnol. Oceanogr.*, 38(4), 775–797.
- Williams, M. W., J. S. Baron, N. Caine, R. Sommerfeld, and R. Sanford (1996a), Nitrogen saturation in the Rocky Mountains, *Environ. Sci. Technol.*, 30(2), 640–646.
- Williams, M. W., M. Losleben, N. Caine, and D. Greenland (1996b), Changes in climate and hydrochemical responses in a high-elevation catchment, Rocky Mountains, *Limnol. Oceanogr.*, 41, 939–946.
- Williams, M. W., P. D. Brooks, A. Mosier, and K. A. Tonnessen (1996c), Mineral nitrogen transformations in and under seasonal snow in a high-elevation catchment in the Rocky Mountains, United States, *Water Resour. Res.*, 32(10), 3161–3171.
- Williams, M. W., T. Davinroy, and P. D. Brooks (1997), Organic and inorganic nitrogen pools in talus fields and subalpine water, Green Lakes Valley, Colorado Front Range, *Hydrol. Processes*, 11, 1747–1760.
- Williams, M. W., D. Cline, M. Hartman, and T. Bardsley (1999), Data for snowmelt model development, calibration, and verification at an alpine site, Colorado Front Range, *Water Resour. Res.*, 35(10), 3205–3209.
- Williams, M. W., E. Hood, and N. Caine (2001), Role of organic nitrogen in the nitrogen cycle of a high-elevation catchment, Colorado Front Range, *Water Resour. Res.*, 37(10), 2569–2581.
- Winstral, A., K. Elder, and R. E. Davis (2002), Spatial snow modeling of wind-redistributed snow using terrain-based parameters, *J. Hydro-meteorol.*, 3(5), 524–538.
- Wolfe, A. P., J. S. Baron, and R. J. Cornett (2001), Anthropogenic nitrogen deposition induces rapid change in alpine lakes of the Colorado Front Range (USA), *J. Paleolimnol.*, 25, 1–7.

F. Liu, M. W. Williams, and N. Caine, INSTAAR, University of Colorado, Campus Box 450, Boulder, CO 80309-0450, USA. (fengjing@snobear.colorado.edu)